L·GARDE
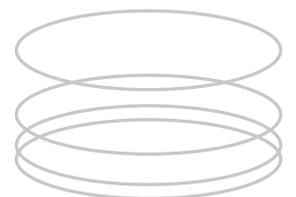
SMART SPACE TECHNOLOGY

Inflatable Concentrators for Solar Propulsion and Dynamic Space Power

G. Grossman, G. Williams

Inflatable Concentrators for Solar Propulsion and Dynamic Space Power[1]

G. Grossman

G. Williams

L'Garde, Inc.
Tustin, CA 92680

This paper describes the development of an inflatable concentrator for solar propulsion, providing the source of heat to a hydrogen engine aboard the Solar Rocket. The latter is a device designed to carry payloads from a low earth orbit (LEO) to a geosynchronous orbit (GEO) at significant mass savings in comparison to chemical propulsion; it involves two lightweight parabolic reflectors in an off-axis configuration focusing solar radiation into the absorbers of the engine, which causes the emission of a hot hydrogen jet. Each of the reflectors has an elliptical rim with a 40 m major axis, providing heat to the propellant sufficient to produce about 40 lbs. of thrust. The same concentrator concept is contemplated for space power application-to focus solar radiation on a conversion device, e.g., a photovoltaic array or the high temperature end of a dynamic engine. Under the present project, a one-fourth scale, 9 × 7 m off-axis inflatable concentrator has been under development as a pilot for the full-scale flight unit. The reflector component consists of a reflective membrane made of specially designed gores and a geometrically identical transparent canopy. The two form together an inflatable lenslike structure which, upon inflation, assumes the accurate paraboloidal shape. This inflatable structure is supported along its rim by a strong, bending-resistant torus. The paper describes the development of this system including the analysis leading to determination of the gore shapes, the reflector membrane design and testing, the analysis of the supporting torus, and a discussion of the effects of the space environment.

1 Introduction

Solar concentrators for use in space have received growing attention in the past few years in view of their many potential applications. Among those, perhaps the most important ones are space power generation and solar propulsion. In the former, the concentrator is used to focus solar radiation on a conversion device, e.g., a photovoltaic array or the high temperature end of a dynamic engine; in the latter, concentrated solar radiation is used to heat a low molecular weight gas, thereby providing thrust to a solar rocket.

Figure 1 illustrates the Solar Thermal Rocket (references [1-3]). In this propulsion scheme, solar energy is reflected by the large parabolic mirrors toward the rocket body, where hydrogen fuel is heated to a very high temperature and exhausted through a nozzle. Table 1 compares solar propulsion with a number of other schemes, for delivering a payload of the same initial mass from the Low Earth Orbit (LEO) of the space shuttle to Geosynchronous Earth Orbit (CEO) [4]. It is evident that solar propulsion is potentially capable of delivering specific impulses nearly double those of current chemical propulsion. The thrust levels are an order of magnitude greater than those attainable by an electric arcjet thruster. The solar rocket offers the mission planner a viable alternative between the high payload-long trip time of an arcjet propulsion device and the relatively low payload-short trip time of the chemical system.

Another application of spaceborne solar concentrators is for power generation [5]. Future missions in space will require abundant power for use on satellites. While conventional photovoltaics have been used in the past and provide a reliable source of power, they do have several drawbacks. Their low efficiencies make it necessary to use large areas of cells, requiring extendible hard structures for support. These large structures make for a complex deployment scheme as well as a high system weight. Another drawback is that the large area required for the low efficiency cells will create significant drag for satellites, especially in Low Earth Orbit (LEO). Solar Dynamic Power Systems (SDPS) offer a viable alternative to photovoltaics, with lower system weight and drag area. These power systems typically consist of large parabolic reflectors that focus solar radiation into a receiver where the high intensity heat is collected. This heat is then used to generate mechanical power using a Brayton, Rankine, or Stirling cycle engine. The lower system weight and area is mainly due to the higher efficiency of dynamic power systems; for a given area of collector surface, more energy is generated with the dynamic power system than with photovoltaics.

Currently, material tests and system designs are being con-

Table 1 Performance Comparison of Different Propulsion Schemes [4]

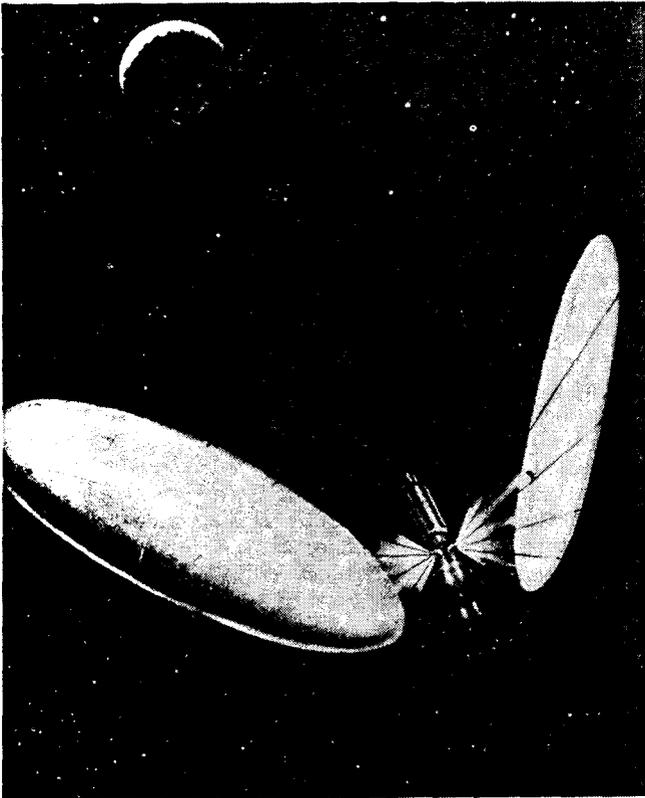|	Arcjet	Nuclear	Solar	Chemical (LH$_2$ – LO$_2$)
Specific impulse (impulse per unit mass) (sec)	1,000	910	872	460
Mass to GEO (lbm)	15,500	36,000	33,000	20,000
Thrust (lbf)	0.5	15,000	64	500
Trip time (days)	103	<1	20	<3
Initial mass (lbm) at LEO	62,000	62,000	62,000	62,000

Fig. 1 Illustration of the solar rocket system (courtesy of Rocketdyne Div., Rockwell International Corporation)
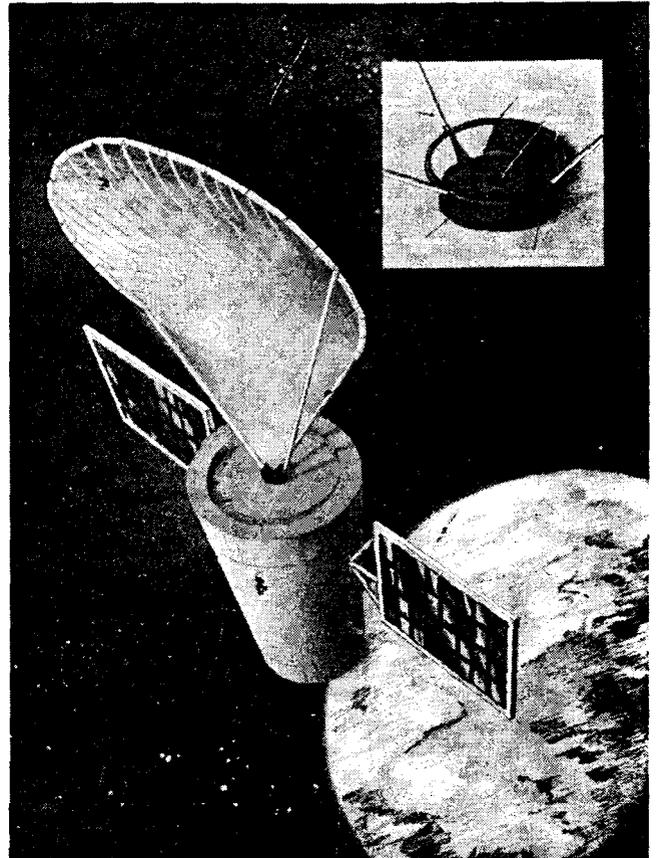

Fig. 2 Inflatable solar reflector for satellite power system

ducted leading to the development of a SDPS for satellite power [6]. The baseline system consists of an off-axis segment of a paraboloidal dish with approximate dimensions of 7 x 9 m (Fig. 2). The concentration ratio (ratio of concentrated heat flux at engine aperture to solar flux incident on reflector) required by this type of system is on the order of 2,000.

One of the most important objectives in the design of space concentrators is low mass. A promising option for achieving this goal is the use of inflatables, the inherent advantages of which have been demonstrated[7,8]. Inflatable space systems invariably require less packaged volume, are lower in weight, and cheaper through both development and production phases than competing mechanically erected systems. The potentially harmful effects of the space environment, including that of micrometeoroids, are much less than originally anticipated since large inflatable concentrators require very low inflation pressure; gas lost through leaks can be easily replaced from a small supply of reserve gas. Inflatables deploy and function very well in space, where the absence of gravity creates extremely low loads. High surface accuracy is obtained due to the constant force provided by the inflatant.

This paper describes the development of an inflatable con-centrator for solar propulsion, providing the source of heat to a hydrogen engine aboard the Solar Rocket. The ultimate system will require two reflectors, each having an elliptical rim with a 40-m major axis, to provide 40 lbs. of thrust to the two engines of the rocket. Under the present project, a one-fourth scale, 9x7 m off-axis concentrator has been under development as a pilot for the full-scale flight unit. The reflector component consists of a reflective membrane made of specially designed gores and a geometrically identical transparent canopy. The two form together an inflatable lenslike structure which, upon inflation, assumes the accurate paraboloidal shape. This inflatable structure is supported along its rim by a strong, bending-resistant torus.

The paper is divided into four sections. First, a description of the concentrator system is given, including the reflector membrane, the outer rim support or torus, and the structural truss. Next, the development of the inflated reflector is discussed. The third section is devoted to the torus, which supports the membrane. The last section discusses the effect of the space environment on these inflatable structures.

2 Concentrator Description

The function of the Deployable Solar Concentrator in the propulsion system of the Solar Rocket is, as explained earlier, to focus solar radiation into the absorber of the hydrogen engine and heat the gas to 2500°C, thereby causing the emission of the hydrogen jet to provide the thrust. The total amount of heat to be supplied by the concentrator is 150 kW, requiring a total reflector projected area of approximately 1500 m². The concentration ratio necessary to achieve the required temperature is about 10,000:1.

Two paraboloidal reflectors in an off-axis configuration are located on either side of the rocket as illustrated in Fig. 1. The reason for this configuration is to avoid an interaction between the reflector and the propellant jet. The off-axis geometry is formed by a plane intersecting a parent paraboloid of revolution (on-axis) of focal length F at some angle to its axis of symmetry. The resulting rim is an ellipse; when viewed along the paraboloid's axis the rim assumes the shape of a circle with a diameter equal to the ellipse's minor axis.

Each reflector is mounted on a truss providing the correct position with respect to the engine. The members of the truss are connected to the reflector outer frame by means of jackscrews, allowing for fine position adjustments, and to the body of the spacecraft by means of a turntable, as illustrated in Fig. 2. The turntable provides one of the two degrees-of-freedom required for pointing the reflector toward the sun irrespective of the direction traveled by the rocket. The other degree-of-freedom is provided by the rocket's roll about its own axis, A control system sensing the location of the concentrated sun spot with respect to the engine aperture employs the jackscrews to adjust the position and to point the reflectors toward the sun as the rocket maneuvers and moves through space. The current sensing concept employs heat/temperature sensors located on the turntable around the absorber aperture. This concept is not final and other methods are being investigated.

Figure 3 illustrates the concentrator, showing its main parts. It consists of two geometrically identical thin membranes forming together a pillowlike structure which, upon inflation, assumes the accurate paraboloidal shape. The two membranes are attached together along the plane, elliptical rim. One membrane has a reflective coating and serves as a concentrating mirror; the other is transparent and serves as a canopy. As mentioned earlier, the dimensions of the prototype reflector presently under development are 7 x 9 m. The inflatable pillow is mounted on a strong, bending-resistant rim support by means of connecting tandems and straps.

The reflector membrane and the canopy are made of very thin films of plastic material. For the current development, 0.25 mil Mylar has been used. The materials for the flight unit will be selected to withstand the damaging effects of the space environment. Each membrane consists of specially designed flat gores seamed together along the edges. When pressurized, the gores undergo an elastic deformation so as to assume the design paraboloidal shape. Note that the uninflated shape is not a paraboloid. A design algorithm has been developed to calculate the shape of the gores as a function of the properties of the material and the inflation pressure. The details of the design process are described in the next section. It should be noted that the inflation pressure required is very low, on the order of 0.0002 psi, and is inversely proportional to the size of the reflector.

The pressure acting over the membrane surface creates a sizable force which must be taken up by the rim support at the edges of the membrane. The rim support contemplated for the present concentrator is an elliptical torus with a circular cross-section. Two alternatives have been considered for the torus design: one is a fully inflatable toroidal tube; the other is a rigidized structure with either a solid or an annular cross-
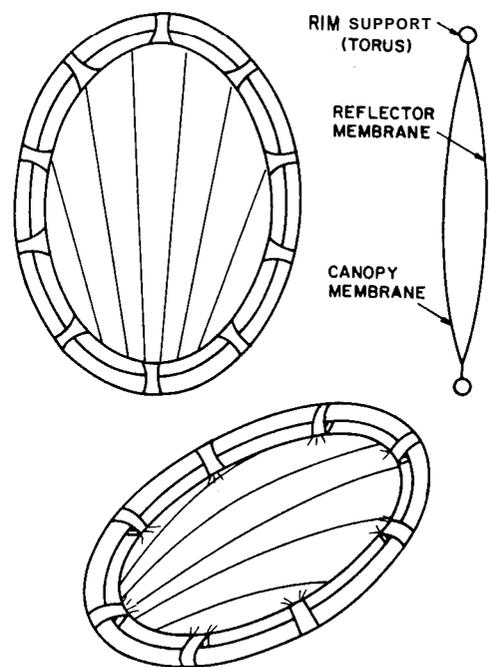

Fig. 3 Schematic description of the deployable solar concentrator

section. The former is preferable from the standpoint of easy deployment and low weight; there is, however, a risk of puncture by micrometeoroids and space debris which could cause significant loss of inflatant. Note that the torus is different in this respect from the reflector, the former requiring much greater pressure than the latter. The rim support analysis and consideration of alternatives will be discussed in detail in Section 4.

The members of the truss connecting the concentrator assembly to the rocket are made of the thin, lightweight aluminum shell. The truss is packaged prior to deployment along with the rest of the concentrator. When inflated, the aluminum shell undergoes plastic deformation which rigidizes it in place. Loss of inflatant from the shell later on will not affect the dimensional stability of the truss. Changes in length of the truss members due to thermal expansion and contractions may be compensated for by the jackscrews.

The concentrator is equipped with a guidance and control system designed to maintain its accurate paraboloidal shape and point it toward the sun, when required, at the correct position with respect to the rocket engine. The former task is performed by sensing the distance between the membranes and adding or venting inflatant, as needed; the latter task is performed by the jackscrews and turntable. Note that the concentrators are in operation only through a fraction of the mission time. The solar rocket path from LEO to GEO involves a series of orbits around the Earth, with relatively short apogee and perigee firings of the engine [3].

Two key components of the Deployable Solar Concentrator-the reflector membrane and the torus-have posed a challenge to development: The former in achieving the high surface accuracy and the latter in providing rigid support while maintaining low weight. The development of these two components is described in the next two sections.

3 Reflector Membrane Design and Testing

To achieve the extreme concentration ratios required by the solar rocket, the reflective membrane must be designed and fabricated with very high accuracy. An analysis was performed using the Concentrator Optical Performance Software
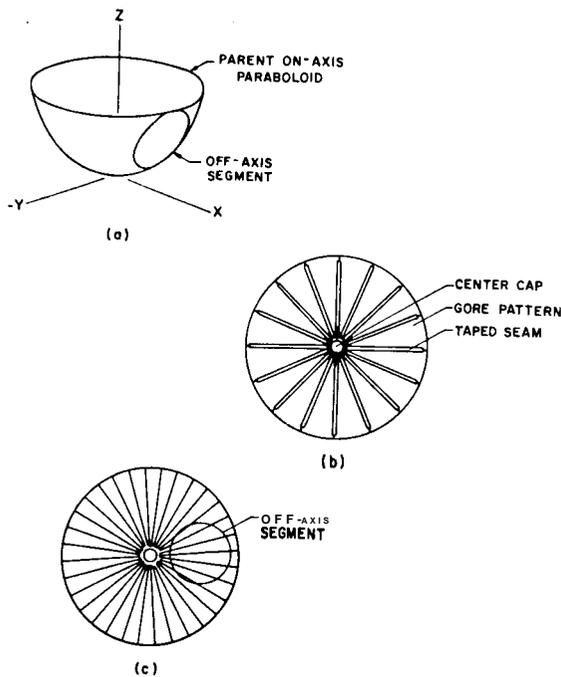
Fig. 4 Geometry of reflector gores: (a) isometric view (b) gore segments (c) top view

(COPS) obtained from the Sandia National Laboratory to determine the effect of surface errors upon concentrator performance [9]. This code takes into consideration the divergence of the solar rays due to the finite size of the solar disk and employs a Monte Carlo ray trace technique which assumes a random distribution of surface inaccuracies over the concentrator surface, within its specified RMS surface accuracy. The code creates a map of power density on the receiver surface and can produce a profile of concentration ratio versus the distance from the center of the receiver. Two modifications to the COPS code were needed in the course of the analysis [9]: First, the axisymmetrical geometry used in the code had to be replaced by the off-axis geometry of the present concentrator; second, the surface deviations found in inflatable paraboloids are not random, but highly ordered [10] ("W" or "M" shaped typically when measured from one side of the paraboloid to the other) due to the tension induced in the membrane by the pressure. The actual concentrator error is a combination of systematic and random errors, the latter resulting partly from the imperfect specularity of the reflector surface. The code was modified to take this into account. In the course of the analysis, the modified code was used to predict the concentrator performance for different combinations of systematic and random error. It was found that a 1.5 mrad random error plus a 2.785 mrad systematic error gave a peak concentration ratio of 10,600 at the center of the receiver and an average of about 10,000 over the entire receiver aperture, which satisfies the engine requirements.[2]

Following the results of the analysis [9], a goal for the concentrator under the present development was set for the slope error not to exceed 1.0 milliradian. The slope error at any point is defined as the angle between the vector normal to the actual reflector surface and that normal to the design paraboloid, at that point. The design problem is to make patterns (gores) of thin film such that when seamed together and

the membrane is pressurized, a three-dimensional paraboloid is formed.

For simplicity, the construction of an on-axis axisymmetric reflector is described first (Fig. 4). In this case the reflector is circular, with the axis of the paraboloid passing through the center of the membrane. Due to the symmetry of the concentrator, all the gore segments are identical. To join the segments, a 3/8 inch wide, 1/2-mil thick tape is used on the back surface of the reflector. The seams are heat sealed; applying a hot iron to the tape melts the adhesive, making a much stronger bond than possible with a pressure-sensitive tape. As shown in Fig. 4(b), the gores do not all meet at the reflector center. Instead, they meet at a circular cap to avoid an excess of overlapping tape from the gore seams.

Determining the shape of the gores is quite complicated. While a complete analysis of the problem is outside the scope of this paper, some theoretical background is presented. The gores are designed to be cut out of a flat, thin plastic sheet. When seamed together and pressurized, they undergo an elastic deformation and assume the design paraboloidal shape. The amount of deformation is a function of the material properties, the inflation pressure, and the geometry. Based on the target paraboloidal geometry with the desired focal length, a "backward" calculation is carried out to give the uninflated shape of the flat gores. The procedure is fairly straightforward when dealing with the uniform properties of a uniform thickness film. The problem then becomes axisymmetrical. We denote arc elements of the inflated paraboloid by dc and ds in the circumferential (hoop) and meridional direction, respectively, and the corresponding ones in the uninflated body of revolution by dc', ds', respectively. Assuming an elastic deformation, we can write:

$$dc = dc'\left(1 + \frac{S_H - \nu S_M}{E}\right) \tag{1}$$

$$ds = ds'\left(1 + \frac{S_M - \nu S_H}{E}\right) \tag{2}$$

where S_H and S_M are the stresses in the hoop and meridional directions, respectively, ν is Poisson's ratio and E is the material modulus of elasticity. S_M and S_H are given by [11]:

$$S_M = pR_H/2t \tag{3}$$

$$S_H = (pR_H/2t)(2 - R_H/R_M) \tag{4}$$

where R_H is the radius of curvature of the surface in the hoop direction, R_M is the radius of curvature in the meridional direction, p is the inflatant pressure, and t is the material thickness. R_H and R_M as well as dc and ds may be expressed in terms of the cylindrical coordinates r, z defining the paraboloid. Thus, for a given pressure, material properties and thickness, four equations are available for the two unknown stresses and the two coordinates defining the uninflated shape.

The problem becomes considerably more complex when considering the effect of the seams, which are much stiffer than the rest of the reflector and reinforce the membrane in parts. Also, the plastic film used to construct the membrane is often slightly unisotropic; with different moduli in the meridional and hoop direction. To solve this more complex problem, a computer code has been developed [10] which helps determine the gore shapes for the membrane. The underlying principle is based on the fact that the material at the gore center (single thickness) will stretch more than the reinforced seams. The outline of each pie-shaped gore can be tailored to provide for this. This design tool has worked quite well; reflectors have been built with slope errors below 3 milliradians RMS [9]. Under the present program, the ability of the code has been extended to handle the off-axis case. This

---

[2] It was later learned that the COPS code in its original form had an error which sometimes led to erroneous results. T. R. Mancini of Sandia National Laboratory indicated to us that this was possibly related to the routine in COPS generating the random Gaussian distribution of solar rays. This routine was replaced by another one but the results did not vary much. Further check of the accuracy requirements using another code may be in order.

is quite a simple extension, when considering that an off-axis paraboloid is actually a portion of a much larger on-axis paraboloid (Fig. 4(c)). A circle is projected over the top view of the dish to determine the points along the gore seams which lie on the border of the off-axis rim.

An accurate gore template and a gore mandrel were fabricated, based on the computer calculations. The template was used to cut the gores out of the flat plastic sheet and to mark their end points. The mandrel was used to position adjacent gore sections when joining them together. The mandrel shape duplicates the profile of the calculated, uninflated shape.

Under earlier programs[9,10] two on-axis paraboloidal inflatable reflectors were developed and tested. The aim was to show that an inflated membrane can be designed and fabricated with a slope error below 3 milliradians RMS. This was in fact achieved; the final tests yielded results better than 2.8 milliradians. Part of the surface inaccuracy is due to the restrictive effect of the seams which is, however, confined to a small area in the vicinity of the seam.

Figures 5 and 6 describe the test set-up for the present, more complex off-axis reflector. A ray tracing technique is used, employing a laser travelling horizontally on an optical bench. The latter is mounted on a steel frame allowing for a vertical change of its position. The frame is positioned with its frontal surface at a 40 deg angle relative to that of the reflector, to simulate the position of the off-axis paraboloid with respect to the sun. Moving the laser on the optical bench and the optical bench on its vertical guides creates a series of parallel beams simulating the solar radiation. The beam can impinge upon any part of the reflector membrane, and is subsequently reflected to a plane focal screen. The traces of the reflected rays on the screen form a series of data points. The accuracy of this method based on the size of the laser image on the screen, and its distance from the screen, was estimated at 0.5 milliradian. Reflector accuracy is determined by a data reduction code based on the positions of the incident and reflected beam relative to the reflector. The data was reduced for the first test article, a subscale 2 x 3 meter membrane, showing very good results. The slope error distribution over the reflector surface is described in Fig. 6. The RMS slope error is approximately 3 milliradians for this case.

4 Rim-Supporting Torus

The pressure acting over the surface of the reflector and canopy membranes creates a sizable force which must be taken up by the rim support at the edge. The rim support-a torus in this case-must have not only the strength to carry this load but also the rigidity to resist deformation and allow the membrane to maintain its accurate shape. The first step toward the design of the torus consisted, therefore, of a load and deformation analysis [12,13]. A complete description of the analysis is beyond the scope of this paper; a summary of the methodology and the results is given as follows.

Earlier work on structural problems in rim supports of inflatable membranes has concentrated largely on circular rings. Due to the axial symmetry, the membrane-applied tension results in a uniform compressive stress in the ring. Murphy [18] gave an excellent description of the experience with circular heliostat frames which have sometimes shown signs of buckling out of the plane of the ring. This buckling results from insufficient strength against bending in a circular ring designed to hold no more than a uniformly distributed compressive load. In the present off-axis case, the rim support is not circular but elliptical; it is subject to a nonuniform load and therefore must be designed to carry bending in the plane of the ellipse. The resulting toroidal cross-section would make it more than sufficiently resistant to out-of-plane buckling.

In calculating the load, the forces transmitted by the membranes to the rim were first evaluated. Despite the complex off-axis geometry, calculation of the forces may be simplified by considering the fact that the off-axis membrane forms part of a parent axisymmetrical paraboloid. The meridional and
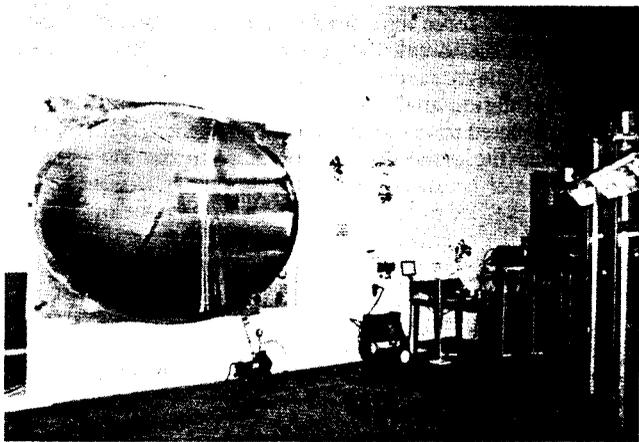

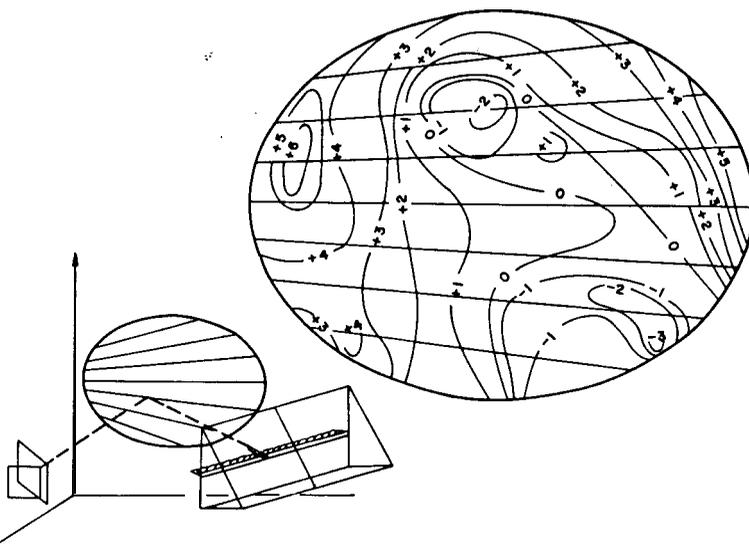**Fig. 5   Test apparatus for reflector membrane**

Fig. 6   Schematic description of test apparatus and test results (slope errors are given in milliradians)
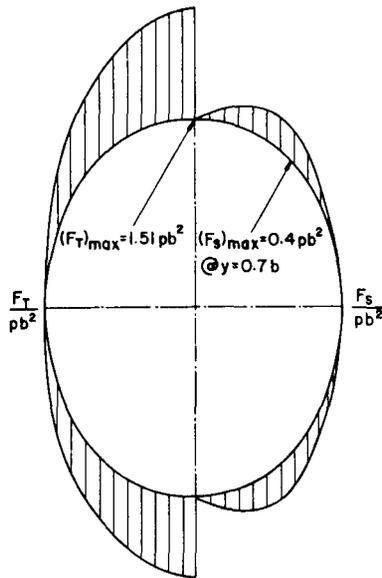
Fig. 7 Internal forces distribution along the elliptical rim in the normal (right) and tangential (left) directions

Fig. 8 Moment distribution (left) and deformation distribution (right) along the elliptical rim

circumferential stress distribution in the latter may be calculated using equations (3) and (4), with the radii of curvature evaluated from the parabolic geometry. Then, the forces transmitted to the rim support are calculated by applying those stresses at points along the off-axis elliptical rim (recall that the off-axis paraboloid is formed by intersecting the parent paraboloid by an inclined plane). The analysis [12] has shown the tension per unit length of rim exerted on the rim support by the membranes to be on the order of (pb), where p is the inflation pressure and b is half the major axis of the ellipse-a characteristic dimension of the rim support. The tension, therefore, increases in direct proportion to the size and to the pressure. Normally, the requirement in designing an inflatable reflector is to maintain some minimum tension in the membrane in order to remove wrinkles and "waviness" from it. Thus, the larger the reflector, the larger the radius of curvature and the smaller the inflation pressure required. For the present 7 x 9 m reflector, the pressure was selected to be 0.0012 psi, based on the gore design. In the ultimate 31×40 meter unit, the pressure would be about four times lower. For the geometry of the Deployable Solar Concentrator, the maximum force per unit area exerted by the two membranes on the rim is 2 x 1.39 (pb) and is almost normal to the rim. For the 7×9 m concentrator this maximum force amounts to 0.6 lbf/in.

The forces transmitted to the rim support create in it internal compression and shear forces; in the case of an off-axis geometry, the lack of symmetry in the torus also causes bending moments. The internal forces and moments may be calculated by a free body analysis of sections of the torus, taking into consideration the membrane-applied forces. The analysis [12] has shown the internal forces to be on the order of (pb^2) and the internal moments-on the order of (pb^3). Figure 7 describes the internal force distribution along the rim for the geometry of the Deployable Solar Concentrator. Shear forces, normal to the rim, are shown on the right part of the ellipse and compression forces, tangential to the rim, are shown on the left. It is evident that the compression forces are considerably larger, at any point, than the shear forces. Thus, with (pb) approximately constant, the shear and compression increase with the first power of the reflector size and the moments-with the square of the reflector size; the stresses resulting from these loads are dominated by bending. The analysis has yielded the force and moment distribution along the torus. The largest compression force and bending moment
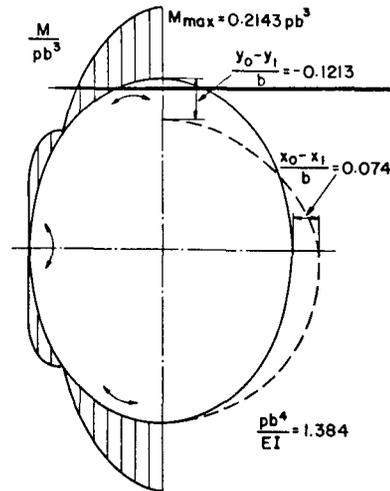
occur at the top end (farthest from the focus). For the particular geometry of the Deployable Solar Concentrator, they are 1.50pb^2 and 0.21pb^3, respectively. In the 7x9 meter concentrator, taking into consideration the effect of both the reflector and canopy membranes, the maximum compression force is 116.5 lbf and the maximum bending moment is 2935 lbf-in.

Knowing the force and moment distribution in the torus makes it possible to calculate the deformation, based on the properties of the torus material and its cross-section geometry. In the deformation analysis [13], a differential element of the torus is subjected to the loads calculated earlier [12]. Both the bending and the compression contribute to the deformation although the effect of the former is dominant. Assuming the deformations to be purely elastic, we can calculate the change in length of the element due to the compressive force and its compression resistance (EA), and the change in its radius of curvature based on the bending moment and the bending resistance (EI). Here, E is the modulus of elasticity of the torus material, A is its cross-section area, and I is its moment of inertia. Neglecting the effect of compression, the analysis shows the deformation to be on the order of (pb^5/EI). With (pb) approximately constant, the deformation increases with the fourth power of the size. The deformation distribution along the torus has been calculated by integrating the results for the differential element over the entire torus length [13]. The maximum deflection occurs at the top, along with the largest moment and compression force.

Figure 8 shows the moment distribution (left) and deformation distribution (right) along the elliptical rim. The moment, normalized with respect to (pb^3), reverses direction, as shown, between points at the end of the major and minor axis. The deformation is calculated, with respect to the point, along the ellipse closest to the apex of the parent paraboloid.

The above results have been used to select a torus cross-section to provide both the necessary strength and rigidity. As mentioned earlier, two alternatives have been considered: one is a fully inflatable structure; the other is a rigidized structure. A fully inflatable torus has a clear advantage in ease of deployment and light weight. It consists of a toroidal tube, made of a strong, flexible material which can be folded and packaged into a small volume when uninflated. Several materials were considered for this purpose with the most promising being a coated Kevlar fabric. The pressure required for the inflation of the torus is considerably greater than that for the reflector in order to provide the required strength and rigidity. The one disadvantage of the inflatable concept is the sensitivity to puncture by meteoroids. Due to
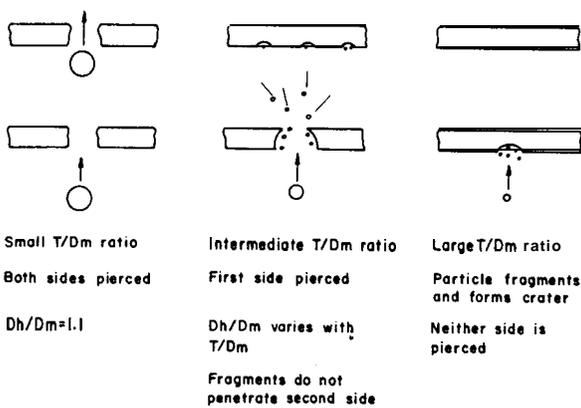
Small T/Dm ratio

Both sides pierced

Dh/Dm=1.1

Intermediate T/Dm ratio

First side pierced

Dh/Dm varies with T/Dm

Fragments do not penetrate second side

Large T/Dm ratio

Particle fragments and forms crater

Neither side is pierced

Fig. 9   Meteoroid model-three regimes of particle size and their effect

the high pressure inside, the leak rate may be prohibitively large.

Under the rigidized concept, a collapsible structure is envisioned which can be packaged along with the reflector prior to launch and inflated in space. Once deployed, the toroidal structure is rigidized in place such that the loss of inflatant at a later time no longer affects its strength or rigidity. Two possibilities have been considered. In one, a thin toroidal tube is filled with polyurethane foam, produced in place from its two liquid monomer components, to form either a solid or an annular cross-section. In the other, the torus is made out of a gelatin-and-water-saturated fabric, which turns rigid as the water evaporates out of the gelatin. At this point, a final decision on which alternative to use has been postponed pending further evaluation.

5 Effects of Space Environment

A number of environmental concerns exist with any spaceborne object. Among the most important are the effects of micrometeoroids, atomic oxygen, and UV radiation. Of those, the ones of greatest potential hazard to inflatable structures are micrometeoroids.

In the past, inflatable structures have not been considered for fear of puncture by micrometeoroids and man-made debris. Their large size makes an easy target for these high velocity particles. However, while most space design requirements seek ultimate reliability through very limited puncture, the thinking behind inflatables is completely opposite. Rather than protect the structure with heavy bumpers, it is made lighter in weight, allowing full puncture by meteoroids and replacing the gas that leaks with a small supply of stored inflatant. The full advantage of this approach becomes evident when considering that the larger the structure size, the lower the inflation pressure. With an object in the space vacuum, the inflation pressures are extremely low, on the order of 10^{-5} psia. The inflated volume is in fact so rarefied that the leakage is dominated by free-molecular flow.

A model has been developed to estimate the effect of meteoroid puncture [6]. It takes into consideration two factors: (1) the meteoroid environment, and (2) the meteoroid damage mechanism. The same model has been used to predict damage to other space structures [14]. For the present analysis, the environment for GEO is used since the Solar Rocket spends little time in the heavily cluttered LEO. The flux equations are given below[15]:

for $-12 \le \mathrm{LOG}m \le -6$

$$\mathrm{LOG}N = -14.339 - 1.584\mathrm{LOG}m - 0.063(\mathrm{LOG}m)^2 \qquad (5)$$

for $-6 \le \mathrm{LOG}m \le 0$

$$\mathrm{LOG}N = -14.41 - 1.22\mathrm{LOG}m \qquad (6)$$

where m is the mass of the meteoroid in grams, LOG refers to base 10 logarithms, and N is the number of particles of mass m or greater, per square meter per second of exposure time. To convert meteoroid mass to size, the meteoroids are estimated to have a specific gravity of 0.5. Debris is excluded in this case since GEO is relatively unpolluted.

The meteoroid damage mechanism was also taken from reference [15]. In all cases of puncture, the diameter of the hole created is larger than the meteoroid. This is based on tests performed prior to the Apollo missions, and also on recent tested performed specifically on thin films. The damage to the film is a function of the material-thickness-to-meteoroid-diameter (T/D_m) ratio.

For low values of T/D_m (large meteoroids) the hole diameter created is slightly larger (1.1 times) than the meteoroid diameter. This is referred to as the "cookie cutter" region. The particle passes through the film without breaking up and continues to pierce the "back" side of the balloon.

In the intermediate range of the T/D_m ratio, the meteoroid and the material break up upon impact and a hole is created which is much larger than the particle, by an amount dictated by the T/D_m ratio. In this case, most of the particle's energy is lost due to impact and the fragments do not continue to pierce the second side of the balloon.

For very high values of the T/D_m ratio, (large material thickness) the particle does not have sufficient energy for complete penetration. Instead, a crater is formed in the material which will affect the local material strength, but there will be no passage of the gas from the inside to outer space. The additional effects of the stress due to cratering are unknown at this time and are not factored into the analysis.

A summary of the meteoroid damage model is given in Fig. 9.

Combining both environment and the damage model yields the inflatant loss. The gas loss from the solar rocket reflectors for the first 30 days in space has been calculated to be only 1.3 pounds.

The most prevalent substance in Low Earth Orbits is atomic oxygen, which tends to degrade any organic or highly oxidizing metal structure in LEO, partly due to a chemical reaction, partly due to mechanical impingement. Coatings are presently being developed to protect hard surfaces from atomic oxygen degradation [16]. Similar coatings may be available in the future for protection of thin films.

The films and coatings of spaceborne solar concentrators are chosen to best protect it from UV radiation degradation. Mylar tends to degrade and crumble due to space exposure. Therefore, while Mylar has been used for the ground-based reflector development tests, a material more resistant to UV such as Kapton will be used in flight. Transparent Teflon will be used for the canopy. An additional advantage to the Teflon is that it is the least reactive film to atomic oxgyen [17].

6 Conclusion

An inflatable prototype for the Deployable Solar Concentrator has been developed. Detailed analyses have been conducted on different aspects of the inflatable off-axis concentrator-gore design, surface accuracy, rim support strength, and deformation. The tests conducted to date on a subscale 2 x 3 meter model are encouraging. The studies show the inflatable reflector to be a viable concept and an attractive alternative to rigidized structures for space solar concentrators.

References

1 Etheridge, F. G., "Solar Rocket System Concept Analysis," Technical Report No. AFRPL-TR-79-79, Air Force Rocket Propulsion Laboratory, Dec. 1979.

2 Shoji, J. M., "Solar Rocket Components Study," Technical Report No. AFRPL-TR-84-057, Air Force Rocket Propulsion Laboratory, Feb. 1985.

3 Shoji, J. M., and Frye. P. E,. "Solar Thermal Propulsion for Orbit Transfer," AIAA Paper No. 88-3171, Presented at the 24th. Joint Propulsion Conference, Boston, Mass., July 11-13, 1988.

4 Naujokas, J., NASA-Lewis Research Center, private communication, December 1988. Also, J. M. Shoji "Performance Potential of Advanced Solar Thermal Propulsion," AIAA Paper No. 83-1307, presented at the 19th Joint Propulsion Conference, Washington D. C., June 27-29, 1983.

5 Archer, J. S.,and Diamant. E. S., "Solar Dynamic Power for the Space Station," AIAA paper No. 86-1299, Presented at the AIAA/ASME 4th joint Thermophysics and Heat Transfer Conference, Boston, Mass., June 2-4, 1986.

6 Williams, G. T., "Inflatable Solar Concentrators for Satellite Power Systems," L'Garde final report to Martin Marietta Denver Aerospace under Contract RH7-165442, Tustin, Calif., July 1988.

7 Thomas, M., and Friese, G. J., "Pressurized Antennas for Space Radars," AIAA paper No 80-1928-CP, presented at the Conference on Sensor Systems for the 80's, Colorado Springs, Colo., Dec. 2-4, 1980.

8 Williams, G. T., "Inflatables for Lightweight Satellite Applications," presented at the 1st Annual USU Conference on Small Satellites, Logan, Utah, Oct. 7-9, 1987.

9 Veal, G. R., "Highly Accurate Inflatable Reflectors, Phase II," Technical Report NO. AFRPL TR-86-089, Air Force Rocket Propulsion Laboratory. Mar. 1987.

10 Thomas, M., and Veal, G. R., "Highly Accurate Inflatable Reflectors." Technical Report No. AFRPL-TR-84-021, Air Force Rocket Propulsion Laboratory, May 1984.

11 Roark, Raymond, J., *Formulas for Stress and Strain*, McGraw-Hill Book Co., New York, 1971.

12 Grossman, G., "Structural Analysis of Rim Supports for Off-Axis Inflatable Reflectors: Load Analysis," L'Garde Technical Report LTR-87-GG-041, Dec. 1987, (accepted for publication in the *ASCE Journal of Aerospace Engineering*).

13 Grossman, G., "Structural Analysis of Rim Supports for Off-Axis Inflatable Reflectors: Deformation Analysis," L'Garde Technical Report LTR-88-GG-033, Jan. 1989, (accepted for publication in the *ASCE Journal of Aerospace Engineering*).

14 Chittenden, D., Grossman, G., Rossel, E., Van Etten, P., and Williams, G., "High Power Inflatable Radiator for Thermal Rejection from Space Power Systems," *Proceedings, the 23rd Intersociety Energy Conversion Engineering Conference*, Denver, Colo., July 31-Aug. 4, 1988, Vol. 1, pp. 353-358.

15 "Meteoroid Environment Model-1969 (Near Earth to Lunar Surface)," NASA Special Publication SP-8013, Mar. 1969.

16 Gulino, D., "Solar Dynamic Concentrator Durability in Atomic Oxygen and Micrometeoroid Environments," AIAA Paper No. 87-0104, presented at the AIAA 25th Aerospace Sciences Meeting, Reno, Nev., Jan. 12-15, 1987.

17 Leger, L., Visentine, T., and Santos-Mason, B., "Selected Materials Issues Associated with Space Station," *SAMPLE Quarterly, Vol. 18, No. 2, pp. 48-54,* Jan. 1987.

18 Murphy, L. M., "Stretched-Membrane Heliostat Technology," ASME JOURNAL OF SOLAR ENERGY ENGINEERING, Vol. 108, pp. 230-237, 1986.

L•Garde Inc
15181 Woodlawn Avenue
Tustin, CA 92780-6487
www.LGarde.com